Supplemental Material: Charge density wave melting in one-dimensional wires with femtosecond sub-gap excitation

M. Chávez-Cervantes,[1,*] G. E. Topp,[1] S. Aeschlimann,[1]
R. Krause,[1] S. A. Sato,[1] M. A. Sentef,[1] and I. Gierz[1,†]

[1]*Max Planck Institute for the Structure and Dynamics of Matter, Center for Free Electron Laser Science, Hamburg, Germany*

(Dated: June 20, 2019)

Sample preparation

The samples were prepared on a phosphorous-doped Si(111) wafer from CrysTec. The sample has a resistance ranging from 1 to 20 Ωcm and a 1° miscut along the $[\bar{1}\bar{1}2]$ direction. The small miscut angle ensures the growth of indium wires in a single domain [1]. The wafer was annealed to 1100 °C by direct current heating until the pressure in the chamber stayed below 1×10^{-9} mbar. In order to obtain regular steps of mono-atomic height on the (7×7) surface we flashed the substrate to 1260 °C and slowly cooled down to 1060 °C followed by a fast temperature decrease to 850 °C [2]. We repeated this procedure until the pressure stayed below 3×10^{-9} mbar during the 1260 °C flash. Afterwards we deposited around 10 monolayers of indium on the clean substrate at room temperature from an electron beam evaporator and annealed the sample at 400 °C for 5 minutes which produced the desired (4×1) structure. All steps during sample preparation were monitored with low energy electron diffraction (LEED, see Fig. 1).

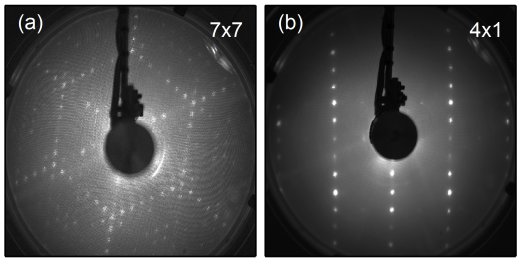

FIG. 1: **LEED pictures.** (a) clean Si(111) (7×7) reconstruction at 58 eV electron energy. (b) (4×1) reconstruction obtained after indium deposition and annealing at 77 eV electron energy.

Tr-ARPES setup

The tr-ARPES setup is based on a Titanium:Sapphire amplifier operating at a repetition rate of 1 kHz to generate synchronized pump and probe pulses. 1 mJ of output power is frequency-doubled in a β barium borate (BBO) crystal and focused into an argon jet to generate high harmonics, producing a broad spectrum of extreme ultra-violet (XUV) light. The 7^{th} harmonic at $\hbar\omega_{\text{probe}} = 22$ eV is selected with a time-preserving grating monochromator [3] and used as a probe pulse for the tr-ARPES experiments. This photon energy is high

enough to reach beyond the first Brillouin zone boundary of the In/Si(111) (4×1) phase and measure the complete band structure of the system.

Mid-infrared pump pulses are generated by overlapping the signal at 1410 nm and idler pulses at 1796 nm from an optical parametric amplifier on a GaSe crystal to obtain pulses at 6.6 μm ($\hbar\omega = 190$ meV) by difference frequency generation. The signal and idler beams are blocked with a long pass filter (Spectrogon LP-4860) that transmits light with a wavelength above 4.86 μm. The wavelength of the generated MIR beam was measured using a Fourier transform infrared (FTIR) spectrometer. The spectrum of the pump pulse is shown in Fig. 2.

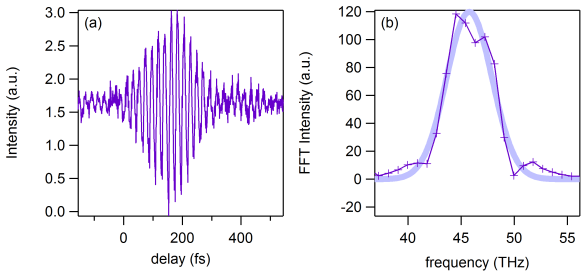

FIG. 2: **FTIR spectrum of pump pulse.** (a) Interference pattern in the time domain. (b) Fourier transform of (a) giving the spectrum of the pump pulse in the frequency domain with a center frequency of 46 THz (6.5 μm).

After excitation of the sample with the pump pulse the time-delayed XUV pulse ejects photoelectrons. Snapshots of the band structure are obtained by dispersing the photoelectrons according to their kinetic energy and emission angle with a hemispherical analyzer and counting them with a two-dimensional detector.

The overall energy and time resolution of the tr-ARPES setup for this experiment were 300 meV and 300 fs, respectively.

Calculation of the peak electric field

We estimate the peak electric field in the surface of the sample parallel to the wires as follows. First we measure the average power P and the spot size d at the sample position. The two-dimensional beam profile of the MIR pump pulse was measured with a Spiricon Pyrocam from Ophir and fitted with a Gaussian to obtain the full width at half maximum d prior to each pump-probe scan. The typical beam size was 1 mm^2. The pump pulse

duration τ is obtained by fitting the time dependence of the LAPE signal (see next section) with a Gaussian the width of which is given by the cross correlation between pump and probe pulses. The probe pulse has a nominal duration of 100 fs. From these parameters we calculate the peak intensity of the pump pulse via

$$I = \frac{4P}{R\tau\pi d^2},$$

where R is the 1 kHz repetition rate of the laser. The incident electric field strength E_i is calculated via

$$E_i = \sqrt{\frac{2I}{c\epsilon_0}},$$

with the speed of light c and the vacuum permitivity ϵ_0. The ratio between the incoming field E_i and the transmitted field E_t is given by the Fresnel equation for p-polarized light:

$$\frac{E_t}{E_i} = \frac{2\cos\theta_i}{n\cos\theta_i + \cos\theta_t},$$

where $n = 3.42$ is the refractive index of the silicon substrate at 6.6 μm, and $\theta_i = 25°$ is the angle of incidence of the light. θ_t is related to θ_i via Snell's law. The field amplitude projected into the surface of the sample along the direction of the wires $E_{t,x}$ can be calculated via

$$\frac{E_{t,x}}{E_i} = \frac{E_t\cos\theta_t}{E_i}.$$

All things considered, the field strength in the surface of the sample in the direction parallel to the wires is given by

$$E_{t,x} = 0.44E_i.$$

tr-ARPES data for all fluences

In Figs. 3 to 5 we present the complete tr-ARPES data used for Figs. 2 and 3 of the main text. Note that the photocurrent for negative pump-probe delays for the high fluence measurements in panel (a) of Fig. 5 shows some remaining intensity in the area where

band m_1 is located in the high temperature phase. We would like to point out that this is commonly observed in tr-ARPES measurements on this material system by us [4] and other groups [5] for pump energies $\geq 1\,\mathrm{eV}$.

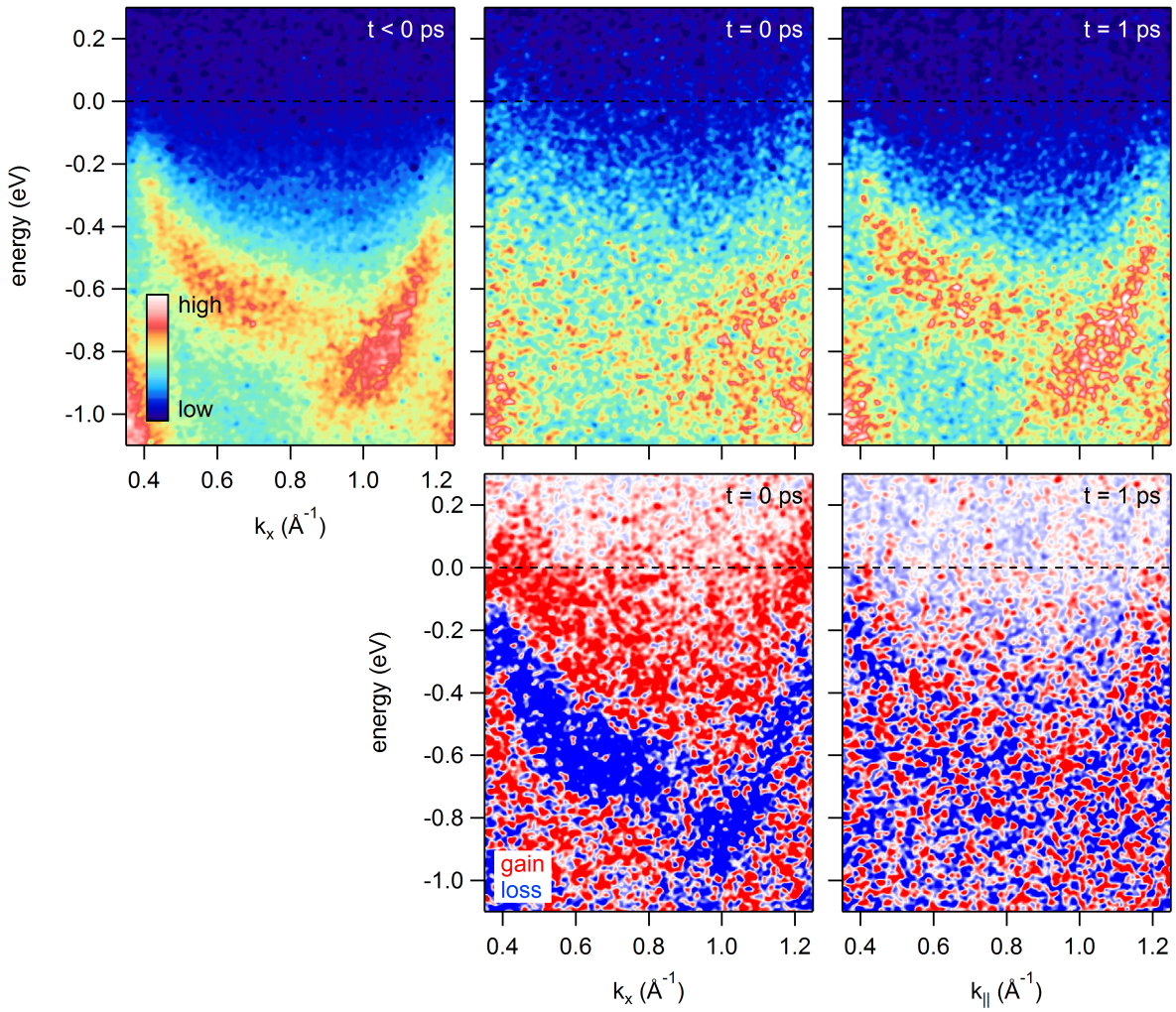

FIG. 3: **tr-ARPES data 0.3 MV/cm.** (a) - (c) photocurrent at various pump-probe delays as indicated in each panel. (d) and (e) pump-induced changes of the photocurrent obtained by subtracting panel (a) from panels (b) and (c), respectively.

Data analysis

We used the following fitting function to extract rise and decay times from the data presented in Fig. 3 of the main text:

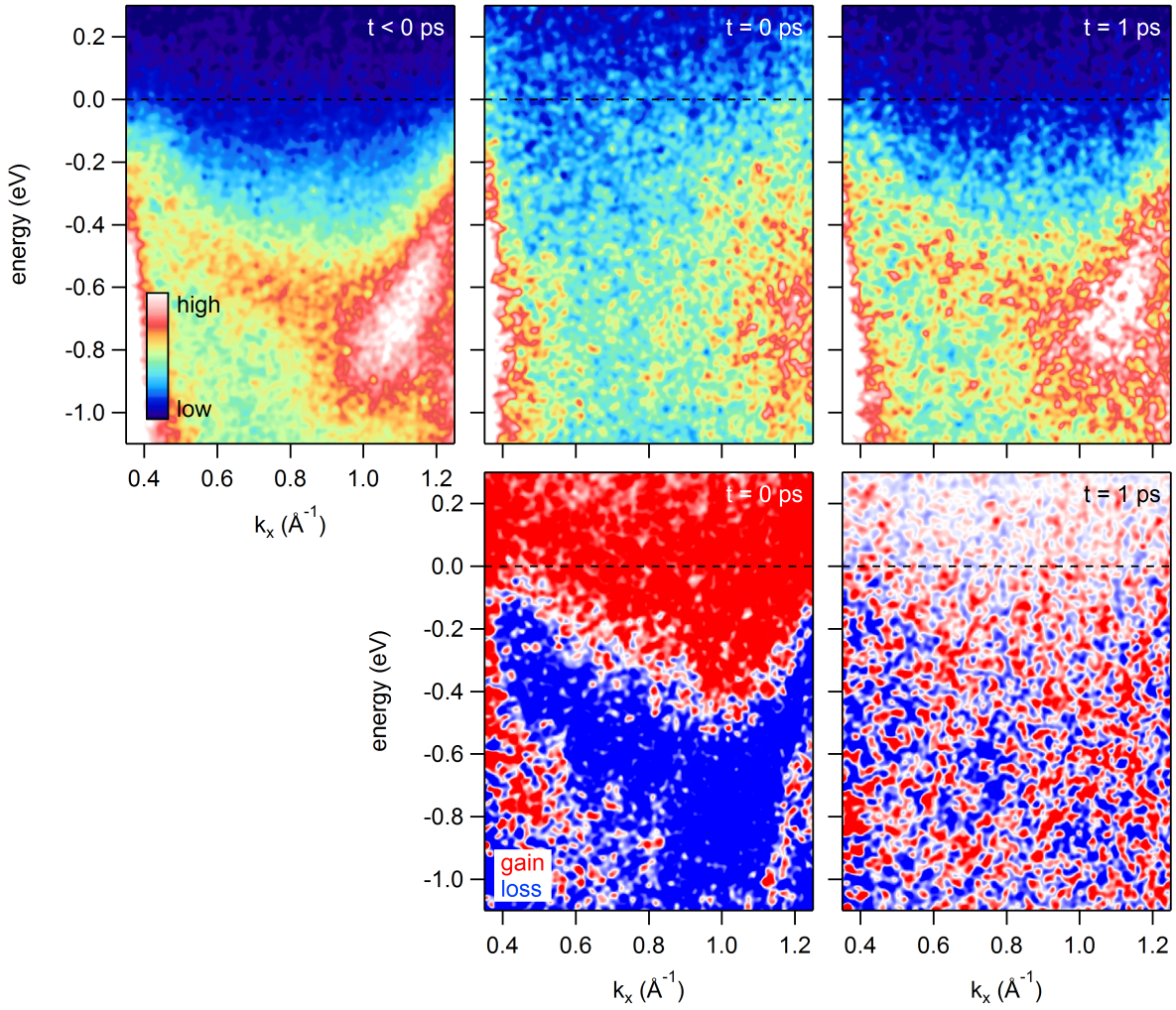

FIG. 4: **tr-ARPES data 0.7 MV/cm.** (a) - (c) photocurrent at various pump-probe delays as indicated in each panel. (d) and (e) pump-induced changes of the photocurrent obtained by subtracting panel (a) from panels (b) and (c), respectively.

$$f(t) = \frac{a}{2}\left(1 + \mathrm{erf}\left(\frac{(t-t_0)\tau - \mathrm{FWHM}^2/(8\ln 2)}{\mathrm{FWHM}\tau/(2\sqrt{\ln 2})}\right)\right)\exp\left(\frac{\mathrm{FWHM}^2/(8\ln 2) - 2(t-t_0)\tau}{2\tau^2}\right)$$

a is the amplitude of the pump-probe signal, FWHM ist the full width at half maximum of the derivative of the rising edge, t_0 is the middle of the rising edge, erf is the error function, and τ is the exponential lifetime. This fitting function is obtained by convolving the product of a step function and an exponential decay with a Gaussian to account for the finite rise time of the signal.

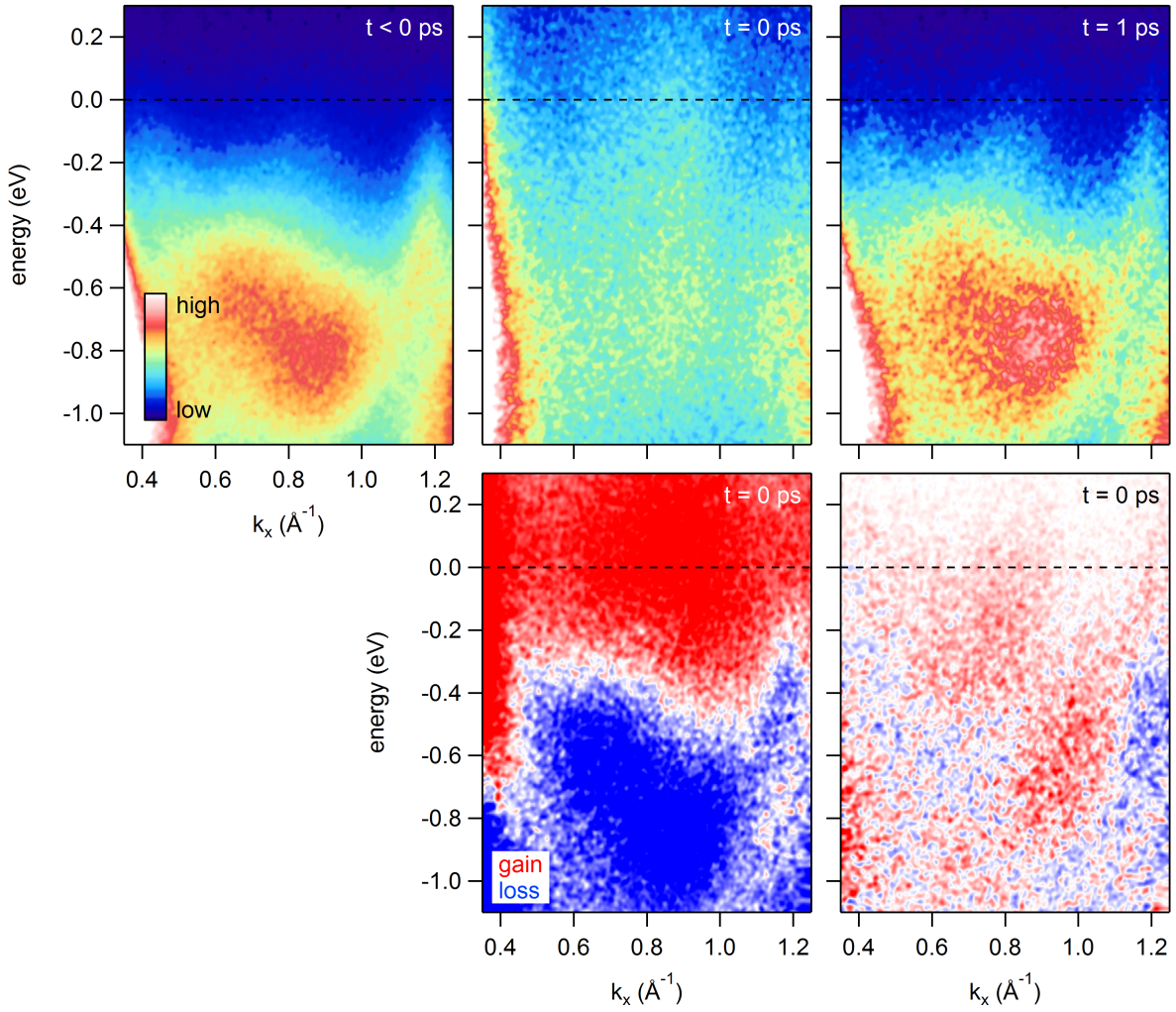

FIG. 5: **tr-ARPES data 0.9 MV/cm.** (a) - (c) photocurrent at various pump-probe delays as indicated in each panel. (d) and (e) pump-induced changes of the photocurrent obtained by subtracting panel (a) from panels (b) and (c), respectively. This is the same data as in Fig. 2 of the main text.

Laser-assisted photoemission

For pump photon energies in the mid-infrared spectral range there is a strong coherent interaction between the pump pulse and the photoemitted electrons in a time-resolved ARPES experiment. This "laser-assisted photoemission" (LAPE) [6], where the kinetic energy of the photoeletron is increased or decreased by integer multiples of the pump photon energy, results in the formation of replica bands in the ARPES spectrum. The number of replica bands that is visible in the ARPES spectrum is determined by the pump field strength: the higher the field, the higher the order of replica bands that appear.

The LAPE effect is particularly strong (absent) when the polarization of the pump pulse is parallel (perpendicular) to the direction in which the photoelectrons are detected. In the present experiment there is a significant component of the pump field along the direction of the detected photoelectrons which means that LAPE dominates the pump-probe signal in the presence of the pump pulse at $t = 0\,\mathrm{ps}$.

In Fig. 6 we provide evidence that the pump-probe signal at $t = 0\,\mathrm{ps}$ in Fig. 2b of the manuscript is given by the formation of replica bands. Figure 6a shows the photocurrent at negative pump-probe delay at room temperature in the metallic phase. Figure 6b shows the pump-induced changes at $t = 0\,\mathrm{ps}$ for pump pulses at $\hbar\omega = 170\,\mathrm{meV}$ for different field strengths of 0.16 MV/cm, 0.30 MV/cm and 0.44 MV/cm from top to bottom, respectively. In order to simulate the pump-probe signal we take the spectrum measured at negative delay and shift it up and down in energy by integer multiples of the pump photon energy. The simulated differential spectra are shown in Fig. 6c. In Fig. 6d we show selected measured (red) and simulated (black) energy distribution curves to show the excellent quantitative agreement. The experimental data is well reproduced with first order replica bands for a field strength of 0.16 MV/cm, first and second order replica bands for a field strength of 0.30 MV/cm, and first, second, and third order replica bands for a field strength of 0.44 MV/cm.

Keldysh parameter

The Keldysh parameter is given by

$$\gamma = \frac{2\pi\nu\sqrt{2m^* E_{\mathrm{gap}}}}{eE},$$

where ν is the frequency of the pump, m^* is the effective mass, $E_{\mathrm{gap}} = 300\,\mathrm{meV}$ is the size of the band gap, e is the charge of the electron, and E is the peak electric field. The effective mass m^* is determined from parabolic fits of the valence and conduction band of the (8×2) structure in [7] as

$$\frac{1}{m^*} = \frac{1}{m_{\mathrm{VB}}} + \frac{1}{m_{\mathrm{CB}}}$$

yielding $m^* = 0.08\,m_e$, where m_e is the mass of the free electron. For a field strength of

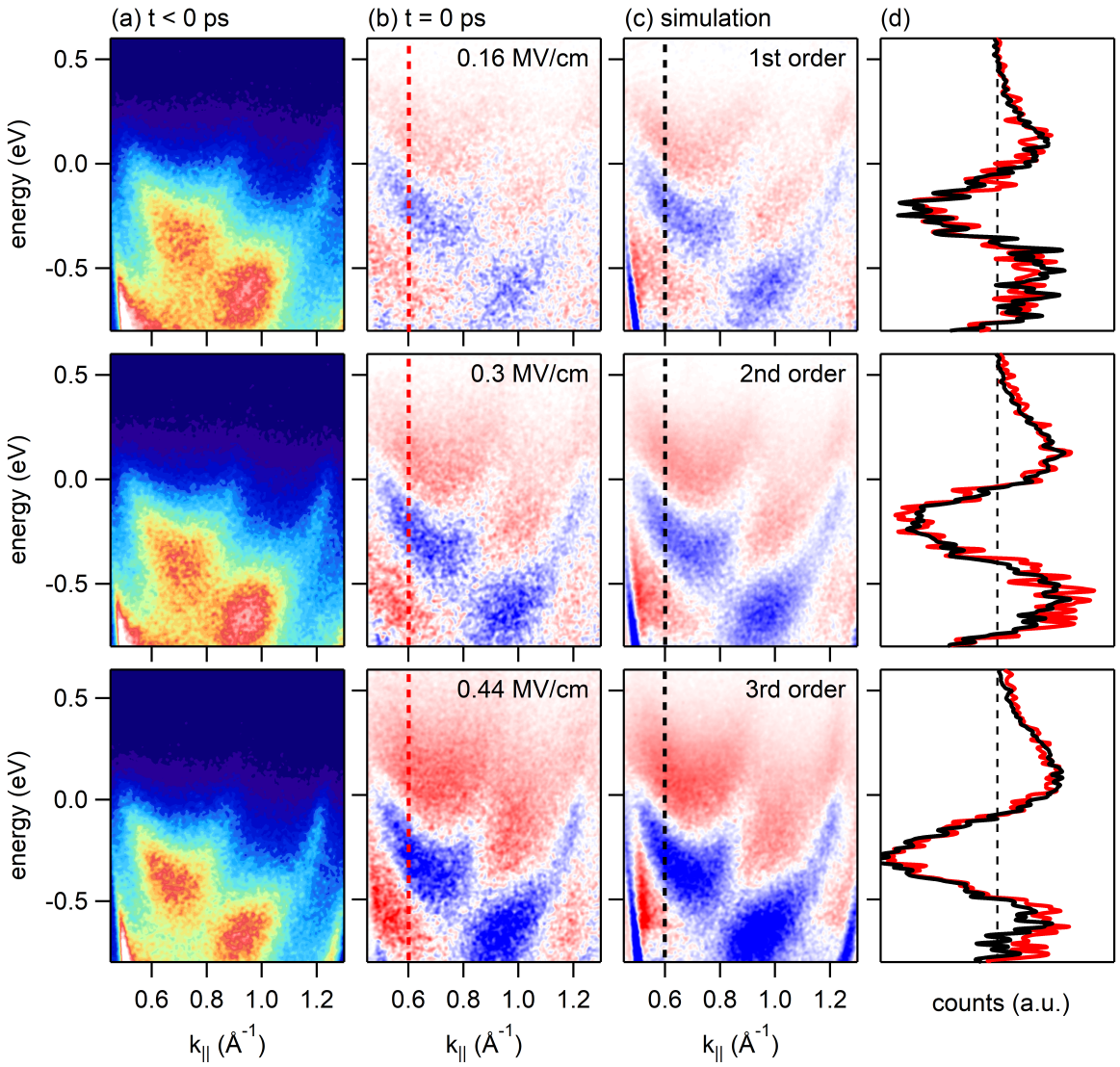

FIG. 6: **Laser-assisted photoemission.** (a) Metallic band structure at negative time delay. (b) Pump-probe signal at $t = 0$ ps with a peak electric field of 0.16 MV/cm (top), 0.30 MV/cm (middle), and 0.44 MV/cm (bottom). (c) Simulated pump-probe signal assuming the generation of first order replica bands (top), first and second order replica bands (middle), and first, second, and third order replica bands (bottom). (d) Direct comparison of measured (red) and simulated (black) energy distribution curves extracted along the dashed line in panels b and c.

0.9 MV/cm we get a Keldysh parameter of $\gamma = 1.6$.

Model

We estimate the critical field strength necessary to melt the CDW by the MIR pump pulse by computing the absorbed energy in a tight-binding model. We use the model Hamiltonian

introduced in the Supplementary Material of [8]. It is of the general form

$$H = \sum_{i,\sigma} \epsilon_i c^\dagger_{i\sigma} c_{i\sigma} - \sum_{\langle i,j\rangle,\sigma} t_{ij} \left(c^\dagger_{i\sigma} c_{j\sigma} + \text{h.c.} \right),$$

where the two terms describe the on-site energies and nearest-neighbour hopping, respectively. Fig. 7 shows a sketch of the corresponding (4×2) unit cell. We use adjusted parameters in order to reproduce the experimentally found band structure of the CDW phase with the reported direct band gap of $\sim 300\,\text{meV}$: $\epsilon_0 = 0.056\,\text{eV}$, $\epsilon_I = 0.089\,\text{eV}$, $t_0 = -0.29\,\text{eV}$, $t'_0 = -0.545\,\text{eV}$, $t_{I1} = 0.1\,\text{eV}$, $t'_{I1} = 0.55\,\text{eV}$, $t_{I2} = -0.104\,\text{eV}$ and $t_{I0} = 0.147\,\text{eV}$.

We apply periodic boundary conditions in the x-direction along the wires to calculate the one-dimensional electronic structure. The band structure in the reduced (4×2) Brillouin zone is shown in Fig. 8. The key feature relevant for the discussion in the main text is the $\sim 300\,\text{meV}$ direct band gap at the reduced zone boundary.

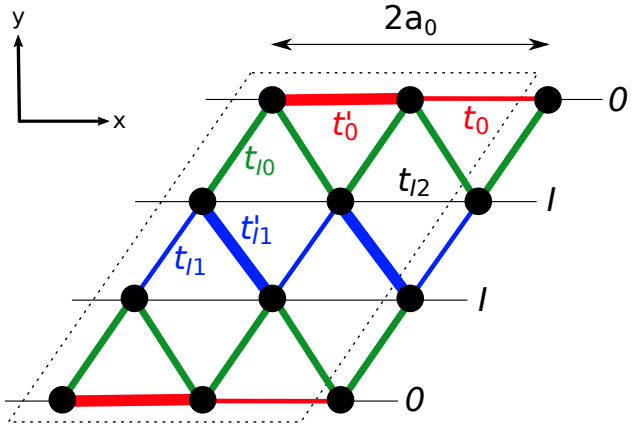

FIG. 7: Schematic sketch of the (4×2) unit cell with different nearest-neighbour hoppings. An increased (decreased) line width indicates an increased (decreased) bond order compared to the metallic (4×1) phase. a_0 is the distance between neighbouring indium atoms.

We set $e = \hbar = c = 1$, sample the one-dimensional reduced BZ with 1024 k-points, and set the electronic temperature to $T = 40\,\text{K}$. The pump pulse is included via a time-dependent vector potential $\mathbf{A}(t) = A_{\max} p_{\sigma_p}(t) \sin(\Omega t) \mathbf{e}_x$ with a Gaussian envelope $p_{\sigma_p}(t) = \exp(-(t-t_0)^2/(2\sigma_p^2))$ and a linear polarization along the wire $\mathbf{e}_x$ via Peierls substitution in the tight-binding model. We use a unitary mid-point propagator of the form $U(t+\delta t) = \exp[-iH(t+\delta t/2)\delta t]$ with a time step of $\delta t = 0.2\,\text{fs}$ to solve the time-dependent Schrödinger equation. The peak electric field strength is related to the maximum of the

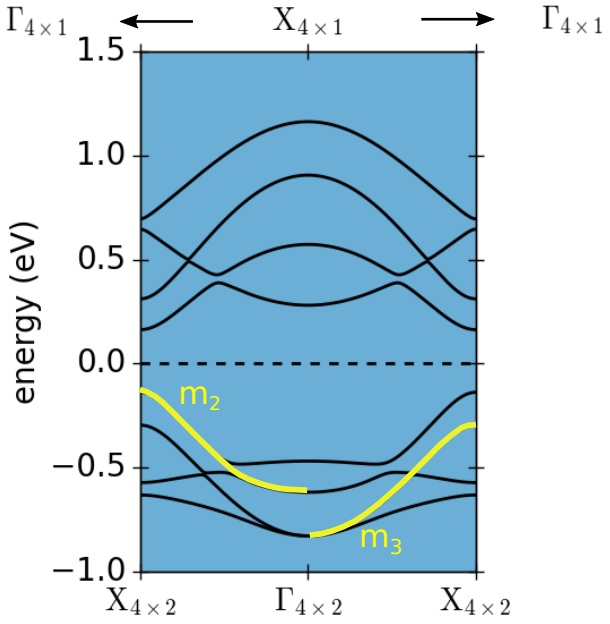

FIG. 8: Band structure of the broken symmetry phase with a 300 meV direct band gap at the X-point of the reduced (4×2) Brillouin zone. The part of the band structure that is visible in the experimental tr-ARPES spectra is highlighted in yellow.

vector potential via $E_{\max} = \Omega A_{\max}$ [9].

As in the experiment, we use a pump photon energy $\hbar\Omega = 190$ meV and a pulse duration of 300 fs at full width at half maximum of the temporal intensity profile. The reported absorbed energy (Fig. 4b of the main text) is then computed from the difference of the total energy per unit cell before and after the pump.

The small discrepancy between the experimental and theoretical threshold field for CDW melting is attributed to uncertainties regarding the size of the gap (literature values range from ∼120 meV [10, 11] to 350 meV [5, 12]) and the condensation energy (literature values range from 47 meV [13] to 66 meV [7] at T = 0 K). Further, both the CDW gap and the condensation energy are temperature dependent. Therefore, both quantities are expected to decrease as a function of time when the pump pulse hits the sample. As the model uses a fixed gap size of 300 meV it is expected to overestimate the field required to melt the CDW. Also, the measured rise and decay times indicate that CDW melting might be incomplete, such that the experimental threshold field of 0.9 MV/cm should be considered as a lower boundary of the actual threshold field.

* Electronic address: mariana.chavez-cervantes@mpsd.mpg.de

† Electronic address: isabella.gierz@mpsd.mpg.de

[1] J. L. Stevens, M. S. Worthington, and I. S. T. Tsong, Phys. Rev. B 47, 1453 (1993)

[2] J.-L. Lin, D. Y. Petrovykh, J. Viernow, F. K. Men, D. J. Seo, and F. J. Himpsel, J. Appl. Phys. 84, 255 (1998)

[3] F. Frassetto, C. Cacho, C. A. Froud, I. C. E. Turcu, P. Villoresi, W. A. Bryan, E. Springate, and L. Poletto, Opt. Express 19, 19169 (2011)

[4] M. Chavez-Cervantes, R. Krause, S. Aeschlimann, and I. Gierz, Phys. Rev B 97, 201401(R)(2018)

[5] C. W. Nicholson, A. Lüke, W. G. Schmidt, M. Puppin, L. Rettig, R. Ernstorfer, and M. Wolf, Science 362, 821 (2018)

[6] G. Saathoff, L. Miaja-Avila, M. Aeschlimann, M. M. Murnane, and H. C. Kapteyn,Phys. Rev. A 77, 022903 (2008)

[7] S.-W. Kim, and J.-H. Cho, Phys. Rev. B 93, 241408(R) (2016)

[8] E. Jeckelmann, S. Sanna, W. G. Schmidt, E. Speiser, and N. Esser, Phys. Rev. B 93, 241407(R) (2016)

[9] M. A. Sentef, M. Claassen, A. F. Kemper, B. Moritz, T. Oka, J. K. Freericks, and T. Derereaux, Nature Comm. 6, 7047 (2015)

[10] H. W. Yeom, K. Horikoshi H. M. Zhang and K. Ono R. I. G. Uhrberg, Phys. Rev. B. 65, 241307 (2002)

[11] Y. J. Sun, S. Agario, S. Souma, K. Sugawara, Y. Tago, T. Sato, and T. Takahashi, Phys. Rev. B 77, 125115 (2008)

[12] S. Chandola, K. Hinrichs, M. Gensch, N. Esser, S. Wippermann, W. G. Schmidt, F. Bechstedt, K. Fleischer, and J. F. McGlip, Phys. Rev. Lett 102, 226805 (2009)

[13] S. Wippermann, W. G. Schmidt, Phys. Rev. Lett. 105, 126102 (2010)